SAND2016-3894C

Compressibility Effects in the Shear Layer over a Rectangular Cavity

Steven J. Beresh,[1] Justin L. Wagner,[2] and Katya M. Casper[3]
Sandia National Laboratories, Albuquerque, NM, 87185

The influence of compressibility on the shear layer over a rectangular cavity of variable width has been studied at a freestream Mach number range of 0.6 to 2.5 using particle image velocimetry data in the streamwise center plane. As the Mach number increases, the vertical component of the turbulence intensity diminishes modestly in the widest cavity, but the two narrower cavities show a more substantial drop in all three components as well as the turbulent shear stress. This contrasts with canonical free shear layers, which show significant reductions in only the vertical component and the turbulent shear stress due to compressibility. The vorticity thickness of the cavity shear layer grows rapidly as it initially develops, then transitions to a slower growth rate once its instability saturates. When normalized by their estimated incompressible values, the growth rates prior to saturation display the classic compressibility effect of suppression as the convective Mach number rises, in excellent agreement with comparable free shear layer data. The specific trend of the reduction in growth rate due to compressibility is modified by the cavity width.

Introduction

Many of the salient physics of aircraft weapons bays are well reproduced by studying simple rectangular cavities. When such a cavity is reasonably short, less than a length-to-depth ratio L/D of approximately 6-8 in subsonic flows [1] and about 10 in supersonic flows [2], the flow is considered to be 'open.' A feedback loop is established between the shear layer impinging upon the rear of the cavity and the aeroacoustic field confined within the cavity walls. This produces longitudinal resonance tones of narrow frequency character and considerable amplitude.

The frequencies of these resonances, though not their amplitudes, are well predicted in simple cavity geometries by a semi-empirical equation attributed to Rossiter [3], though in practice most engineers use the modified form by Heller and Bliss [4]. This equation is dependent upon constants that later were found to be functions of the Mach number [5,6]. As the Mach number becomes significantly supersonic, the physics of cavity resonance appear to shift towards a different acoustic model and agreement with the Rossiter equation may be merely fortuitous [7-9]. Still, many decades of use has shown that the Rossiter equation does a reasonable job of predicting the resonance frequencies of a simple rectangular cavity even if it is not based on sound physics.

Aside from schlieren imaging of waves emanating from cavities, studies of the variation of cavity flow structure with Mach number are uncommon. Murray and Elliott [8] used planar laser scattering to examine large-scale turbulent structures in the shear layer over a two-dimensional cavity at supersonic Mach numbers. Murray et al [10] used particle image velocimetry (PIV) to measure the shear layer and recirculation region for several subsonic and transonic Mach numbers. Though the vast literature of cavity flows covers a thorough range of Mach numbers, no other known studies examined the cavity flowfield structure while varying the Mach number.

Conversely, the effects of compressibility on the turbulence of free shear layers have been well studied. In fact, the subject has received such attention that multiple reviews of it may be found [11-13]. A compilation of numerous

[1]Distinguished Member of the Technical Staff, Engineering Sciences Center, AIAA Associate Fellow, correspondence to: P.O. Box 5800, Mailstop 0825, (505) 844-4618, email: sjberes@sandia.gov
[2]Principal Member of the Technical Staff, AIAA Senior Member
[3]Senior Member of the Technical Staff, AIAA Member

This work is supported by Sandia National Laboratories and the United States Department of Energy. Sandia is a multiprogram laboratory managed and operated by Sandia Corporation, a wholly owned subsidiary of Lockheed Martin Corporation, for the United States Department of Energy's National Nuclear Security Administration under contract DE-AC04-94AL85000.

experiments shows that as the convective Mach number M_c rises, turbulence is suppressed within the shear layer, which has a number of important ramifications. Perhaps most widely observed is a reduction in the growth rate of the shear layer in comparison with its incompressible counterpart and hence a thinner shear layer at equivalent downstream distance [14-17]. Visualizations of the turbulent structure show that the behavior of the shear layer alters once M_c increases past about 0.6, at which point the dominant instability mechanism shifts from the Kelvin-Helmholtz instability to an oblique instability [16, 18]. Simulations support this observation [19].

Velocimetry data of compressible shear layers are rarer, but particularly relevant to understanding the effects of increasing compressibility on turbulence. Laser Doppler velocimetry measurements by Goebel and Dutton [20] showed that the transverse (vertical, in the terms of the present article) component of the turbulence intensity and the turbulent shear stress are considerably reduced with increasing M_c but the streamwise turbulence intensity is minimally reduced if at all. Gruber et al [21] confirmed these trends and added that the spanwise component remains fairly constant. Similar measurements by Elliott and Samimy [22] concurred regarding the transverse turbulence intensity and the turbulent shear stress, but found that the streamwise component of the turbulence intensity diminishes as well. The simulations of Freund et al [23] agree with Goebel and Dutton. Finally, PIV data by Urban and Mungal [24] and Olsen and Dutton [25] are consistent with the Goebel and Dutton viewpoint.

The limited attention to compressibility in the cavity shear layer is unfortunate, as there are several reasons why the shear layer behavior over a cavity can be expected to differ from a free shear layer. Most evidently, in free shear layers, both freestreams are considered uniform and constant, but in a cavity the slower freestream is actually the boundary of the cavity recirculation region, which is not a constant value spatially and likely not temporally either. The Kelvin-Helmholtz instabilities that drive the unsteady free shear layer behavior may be continually excited by the distinct acoustic tones present in cavity resonance [26,27]. Furthermore, impingement of the shear layer on the aft cavity wall is known to affect the shear layer position and therefore change the upstream influence [28,29]. Additionally, the presence of cavity side walls creates spanwise instabilities [30-35] and these have been found to modulate the amplitude of the resonances in a manner that varies with the cavity width [1,36-39]. It already is known that the turbulent structure of compressible free shear layers is influenced by the presence of side walls [40-42] and it is reasonable to infer from this that the cavity walls similarly may alter the turbulence in the shear layer. Given these contrasts, it is unclear whether the compressibility effects so evident in free shear layers will be reproduced in cavity shear layers in a similar fashion or may exhibit differing behavior.

The existing PIV data sets of Beresh et al [43,44] span a freestream Mach number range of 0.6 to 2.5. As calculated later in the present article, this corresponds to an estimated convective Mach number reaching 1.01. Cavity length-to-depth ratio was fixed at 5 while the length-to-width ratio varied from 1 to 5. These data offer an opportunity to explore the influence of compressibility on the turbulence properties of the cavity shear layer and compare the results to those known for free shear layers. Although Beresh et al [43] previously discussed compressibility effects on the cavity shear layer, these were examined in limited detail and only for supersonic conditions. Therefore, the present paper revisits the two earlier data sets with the specific interest of analyzing the compressibility effects.

Experimental Methods

Wind Tunnel and Cavity Hardware

Experiments were performed in Sandia's Trisonic Wind Tunnel (TWT), which is a blowdown-to-atmosphere facility using air as the test gas, whose test section is enclosed within a pressurized plenum. In its transonic configuration, the test section is a rectangular duct of dimensions 305 × 305 mm^2 with interchangeable walls. In the present case, the test section was configured with porous walls on the top wall and one side wall to alleviate non-physical resonances due to wind tunnel duct modes [45]; a solid wall with a window for imaging was installed in the other side of the test section. Despite the non-uniform test section, no evidence of flow asymmetry was detected in either pressure or PIV data. Supersonic experiments were conducted in the TWT's half-nozzle test section, in which the top wall of each supersonic nozzle is retained and a single lower wall extends the inlet contour of the tunnel before fairing into a flat surface at what previously would have been the test section centerline. This provides a flat plate working surface with convenient optical access in a resulting half-nozzle test section of 152 mm high and 305 mm wide.

In the present case, transonic experiments were conducted at Mach numbers 0.60, 0.80, and 0.94, and supersonic experiments were conducted at Mach numbers 1.5, 2.0, and 2.5. Transonic flow conditions were selected to hold the freestream dynamic pressure q_∞ constant to a nominal value of about 33 kPa. Supersonic values of q_∞ were much higher, between 110 and 133 kPa. Previous PIV measurements and Pitot probe surveys have shown that the incoming 99%-velocity boundary layer thickness ranges from about 10 – 15 mm for the entire Mach range of the

present experiments, which is 40-60% of the cavity depth (see below). Since the boundary layer thickness remains within the same range for all cases and this change in Reynolds number is relatively small for a fully turbulent flow, the difference in flow conditions is not expected to be evident in normalized data. Indeed, no effect has been found on the normalized unsteady pressures [46-48], nor does it significantly alter the velocity field or turbulent stresses (based on supplementary data collected as part of the Beresh et al [43] experiment).

The wind tunnel stagnation temperature T_0 is fixed at 321K ± 2K by heating in the storage tanks, and the wall temperature is effectively constant at ambient conditions, T_w=307K ± 3K. Freestream velocities U_∞ were measured from previous PIV experiments as 215, 280, 315, 450, 535, and 605 m/s for the six cases in order of increasing Mach number, estimated to be accurate to within 0.3%.

The finite-width cavity of the present experiments is simply a rectangular pocket in a plate inserted into the lower test section wall. The floor of the cavity is a BK7 glass flat optically coated for anti-reflection at 532 nm to allow the laser sheet for the PIV measurements to enter the test section from below. The cavity has dimensions 127 × 127 mm^2 (5 × 5 inch^2) with a nominal depth of 25.4 mm (1 inch). In practice, the cavity depth was measured to be 25.9 mm (1.02 inch) for the supersonic configuration but achieved the intended dimension of 25.4 mm for the transonic experiments, due to a discrepancy in the crush of a gasket. In addition to the widest cavity dimensions of 127 × 127 mm^2, insert blocks can be bolted against the cavity side walls to reduce the cavity width for additional tests. This was used to create cavities of 127 × 76 mm^2 (5 × 3 inch^2) and 127 × 25 mm^2 (5 × 1 inch^2); the cavity depth was not changed. The respective length-to-width ratios L/W are 1.00, 1.67, and 5.00; the length-to-depth ratio L/D is 4.90 for the three supersonic conditions and 5.00 for the three transonic conditions. These three cavity configurations henceforth will be denoted the 5 × 5, the 5 × 3, and the 5 × 1 cases. The coordinate system was chosen such that x lies in the streamwise direction and y is vertical, positive away from the cavity, with the z coordinate spanwise and right-handed. The origin is the spanwise center of the cavity leading edge.

Particle Image Velocimetry

Two data sets have been collected, both described previously [43,44]. Despite any inference based on publication dates, the supersonic measurements were collected several years prior to the transonic measurements and were somewhat less mature.

In all experiments, the TWT is seeded by a thermal smoke generator using a mineral oil base (Corona Vi-Count 5000) whose output has been previously measured in-situ by tracking the particle response across a shock wave to show a particle size of 0.7 - 0.8 μm. Stokes numbers have been estimated as at most 0.05 based on *a posteriori* measurements of typical cavity shear layer eddies, which is sufficiently small to render particle lag errors negligible.

Supersonic measurements

The supersonic experiment is itself composed of two distinct measurement campaigns. A two-component configuration was used to survey the entire streamwise extent of the shear layer in the cavity along its spanwise centerline by peering partially into the cavity at an angle. This provided the best spatial coverage possible using only two cameras, but the viewing angle introduced an uncorrectable perspective bias error in the vertical velocity component and still could not reach the cavity floor. Conversely, a stereoscopic configuration provided more complete data using the same two cameras in a smaller field of view covering approximately the downstream half of the cavity. Steeper camera angles reached the cavity floor without introducing perspective error owing to the stereoscopic calibration and availability of three components of velocity.

In either configuration, the light source for the PIV system was a frequency-doubled dual-cavity Nd:YAG laser (Spectra Physics PIV-400) that produced 300-400 mJ per beam. The beams were formed into coplanar sheets and directed into the test section from beneath the wind tunnel, then entered the cavity through the window forming its floor. The laser sheet thickness was 1.0 mm and was aligned to the spanwise center of the cavity.

Scattered laser light was collected by interline-transfer CCD cameras (LaVision Imager ProX 4MP) with a resolution of 2048 × 2048 pixels digitized at 14 bits. The two cameras were equipped with 105-mm lenses for the two-component PIV and 200-mm lenses for the stereoscopic PIV; in both cases, the lenses were mounted on Scheimpflug platforms to create an oblique focal plane aligned with the laser sheet. For the two-component configuration, the cameras were placed side by side to survey an extent of the cavity twice as large in the streamwise dimension as in the vertical dimension. The cameras peered down into the cavity at an angle of 11 deg, and an alignment target placed at the laser sheet location was used to produce a calibration that could account for the variable magnification due to the viewing angle.

For stereoscopic data, the cameras viewed the imaging region using compound angles and two-axis Scheimpflug focusing, where half-angles of 12 deg separated the two cameras in the streamwise plane and both were angled identically in the vertical plane at 38 deg to look into the cavity. To increase the vertical angle possible given

optical access restrictions of the TWT, a mirror was rigidly mounted inside the plenum near the top wall to reflect scattered light back towards the cameras at a sharper angle; wind tunnel vibrations were found not to pose a difficulty for modest Reynolds numbers. Stereoscopic camera calibrations were accomplished by placing a single-plane alignment target in the position of the laser sheet, then scanning it through the volume of the laser sheet to acquire seven planes of calibration data, which were calibrated using a polynomial fit.

Data were processed using LaVision's DaVis v7.2. Image pairs were interrogated with an initial pass using 64 × 64 pixel interrogation windows, followed by two iterations of 32 × 32 pixel interrogation windows, which translates into a spatial resolution of approximately 0.8 mm per vector for both measurement configurations. A 50% overlap in the interrogation windows was used as well. The resulting vector fields were validated based upon signal-to-noise ratio, nearest-neighbor comparisons, and allowable velocity range. For all data shown herein, at least 750 vector fields were acquired for each experimental case combining Mach number and cavity width.

Transonic measurements

By the time the transonic experiment was conducted, four cameras were available to survey the entire streamwise extent of the cavity using two stereoscopic fields-of-view. The same laser was used and configured identically, save that the sheet thickness was 1.5 mm.

The four cameras (all LaVision sCMOS, each with a resolution of 2560 × 2160 pixels digitized at 16 bits) were equipped with 200-mm lenses mounted on Scheimpflug platforms viewing the imaging region using compound angles. As in the supersonic experiment, half-angles of 12 deg separated the two cameras of each stereo pair in the streamwise plane and the cameras were tilted in the vertical plane at about 35 deg to provide sufficient angle to view the cavity floor. Again, a mirror rigidly mounted inside the plenum was needed to achieve the desired vertical angle. Stereoscopic camera calibrations were performed identically to the supersonic measurements and self-calibration was used to minimize camera registration error. Data processing was as the supersonic experiment but used DaVis 8.2. About 3000 vector fields were acquired for each case.

Results and Discussion

Turbulence Magnitudes

Representative fields of the turbulence of the cavity flow are shown in Figure 1. Figures 1a and 1b show the streamwise turbulence intensity for the 5 × 5 case at Mach 0.8 and 1.5, respectively. Superposed on these contours are streamlines derived from the mean velocity field to identify the overall flowfield structure. The Mach 0.8 plot is formed from the dual stereoscopic measurements, but the Mach 1.5 plot is a composite of the two-dimensional field of view and the stereoscopic field of view. Combining the field of view in this manner expands the coverage of the cavity from the available measurements. This approach is useful only for the streamwise velocity component as the vertical component is biased for the two-dimensional measurements and of course the spanwise component is absent.

The vertical component of the turbulence intensity is shown in Figs. 1c and 1d for the 5 × 5 cavity at Mach 0.8 and 1.5, respectively. The same streamlines of the mean flow are overlaid on the turbulence intensity contours. In this case, the supersonic data include only the stereoscopic measurements because the vertical component of the two-component measurements is biased due to the camera inclination. The reduced field of view is present for all supersonic cases save the streamwise component in the 5 × 5 cavity.

Field plots such as those shown in Fig. 1 provide the basis to compare turbulence quantities across different Mach numbers and cavity widths, but a more quantitative method is required. The conventional means of comparing velocity statistics between the different Mach numbers would be to extract profiles at various streamwise locations and plot them simultaneously. However, that approach is hampered here by small variations in the cavity flow structure as the Mach number changes, as well as the considerably larger variations as a function of cavity width. Although the fundamental structure is consistent across the range of Mach numbers, the position and size of the recirculation region shifts somewhat as does the peak position of the shear layer, and this variability interferes with a direct comparison of velocity profiles. Moreover, profiles are restricted to a single streamwise location in the flow unless many are provided. A superior approach to investigate the shear layer in the present data set is to locate the maximum value of each turbulence quantity as a function of streamwise location and plot this for each case. This eases comparison between the various conditions and removes the subjective influence of the recirculation region.

Because second-order statistics such as turbulence quantities become noisy as velocity uncertainties are propagated, each data field was filtered prior to locating the local maxima. A median filter was found to be superior to any smoothing algorithms because the former preserves the edges of the shear layer and prevents artificial

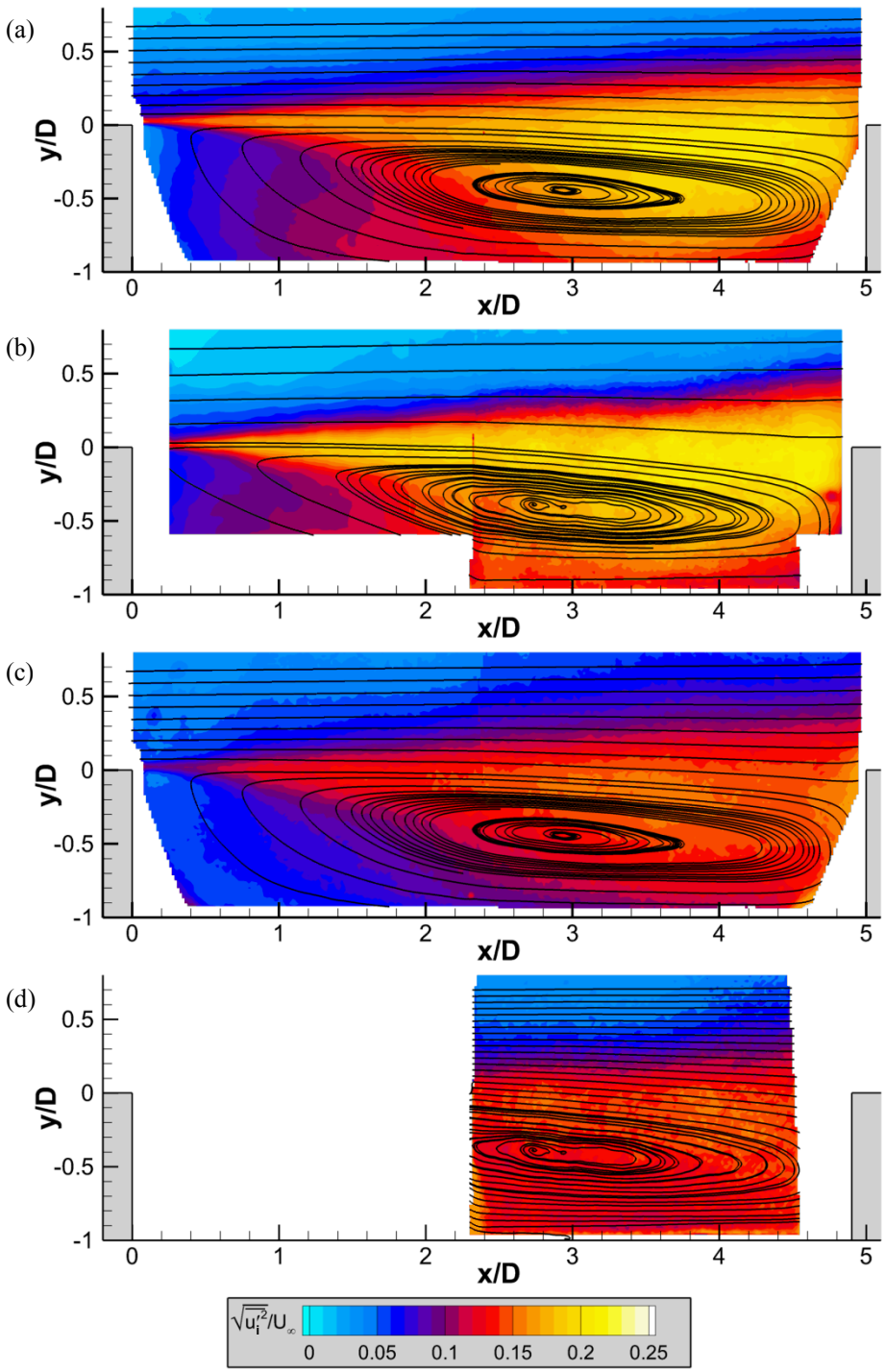

Fig. 1: Turbulence intensity fields for the 5 × 5 cavity with superposed streamlines derived from the mean velocity field; (a) streamwise component at Mach 0.8; (b) streamwise component at Mach 1.5; (c) vertical component at Mach 0.8; (d) vertical component at Mach 1.5.

thickening or reduction of maxima. Subpixel accuracy was obtained by fitting a second-order polynomial in the vicinity of the peak.

Figure 2 shows the maxima for four key turbulence quantities measured in the 5 × 5 cavity: the three components of the turbulence intensity and the primary turbulent shear stress. Compressibility effects are

difficult to detect for this cavity width. The only component to show a clear effect is the vertical turbulence intensity, and this is marginal compared to the uncertainty estimate although its consistency with streamwise position suggests it is significant. Therefore, a small reduction in magnitude of v' with rising supersonic Mach number appears valid. The streamwise and spanwise components actually suggest an increase in magnitude for the supersonic cases, but the lack of a uniform trend as a function of Mach number makes this difficult to interpret. Nothing significant may be extracted concerning the turbulent shear stress in Fig. 2d.

Stronger compressibility effects are observed in the 5 × 3 cavity in Fig. 3. All four turbulence quantities indicate a reduction in magnitude for the supersonic cases as the Mach number rises, to an extent that clearly exceeds the measurement uncertainty. The strength of these trends is considerably greater than anything observed for the 5 × 5 cavity. The strongest impact occurs for v' and $u'v'$.

The results for the 5 × 1 cavity, shown in Fig. 4, are more muddled in comparison to the two wider cavities. This is in part because the mean flow structure of the narrowest cavity differs from the wider configurations [43,44] and in part because a jump in the turbulence magnitudes occurs in the transition from the transonic cases to the Mach 1.5 case. However, when the three supersonic cases are considered independently from the transonic data, it is apparent that the magnitudes of each turbulence quantity fall as the Mach number rises, and that these trends exceed the measurement uncertainty. Therefore, there appears to be a significant compressibility effect (more so than the 5 × 5 cavity in Fig. 2) but it is masked by a second effect that raises the turbulence levels in the supersonic cases. The latter may be an experimental artifact related to the smaller confines of the test section used for the supersonic measurements, though it is unclear why this should occur only for the narrowest cavity. Possibly it is related to the lack of spillage vortices in this case [43,44]. The 5 × 1 cavity also differs in that u' and $u'v'$ appear to peak prior to nearing the aft wall, which is not evident in the 5 × 5 or 5 × 3 cavities, nor does it occur for v' or w'. However, this does not appear to affect the compressibility trends in the three supersonic cases.

Despite the ambiguities, several important points may be gleaned from Figs. 2-4. Compressibility effects are not observed in the three transonic cases but they become possible once Mach 1.5 is reached. A reduction in magnitude of all three components of the turbulence intensity as well as the primary component of the turbulent shear stress occurs as the Mach number is raised. However, this develops only for the 5 × 3 and 5 × 1 cavities. For the 5 × 5 cavity, a significant compressibility effect is observed only for v' and even this is

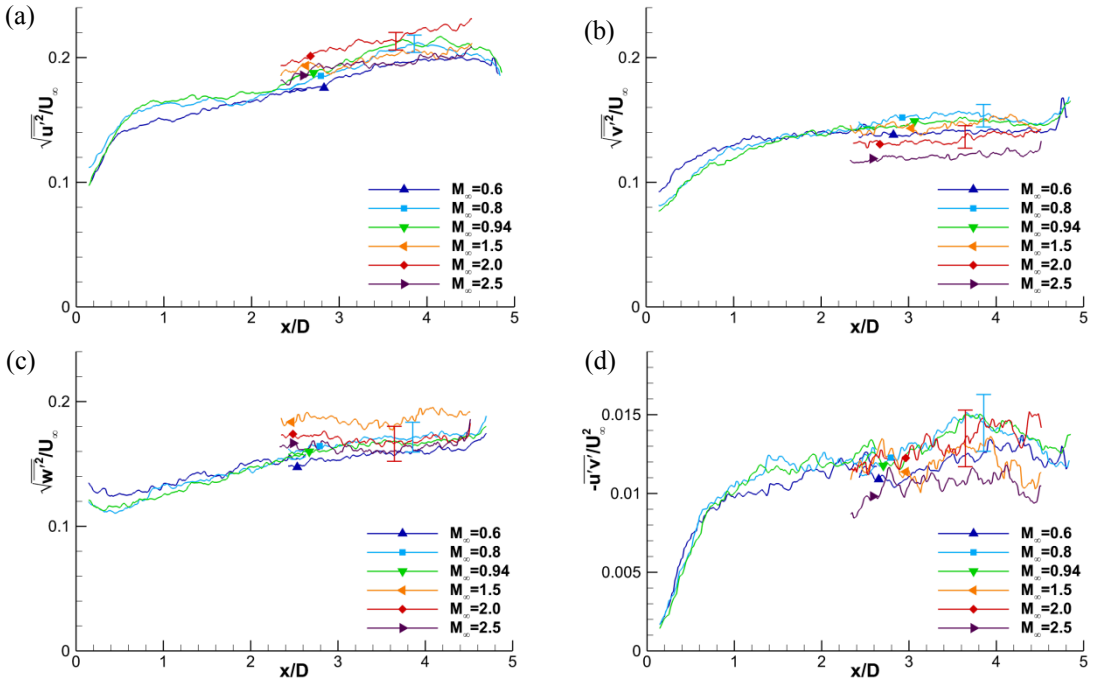

Fig. 2: Maxima of turbulence quantities as a function of streamwise location for the 5 × 5 cavity at all Mach numbers. (a) streamwise turbulence intensity; (b) vertical turbulence intensity; (c) spanwise turbulence intensity; (d) primary turbulent shear stress.

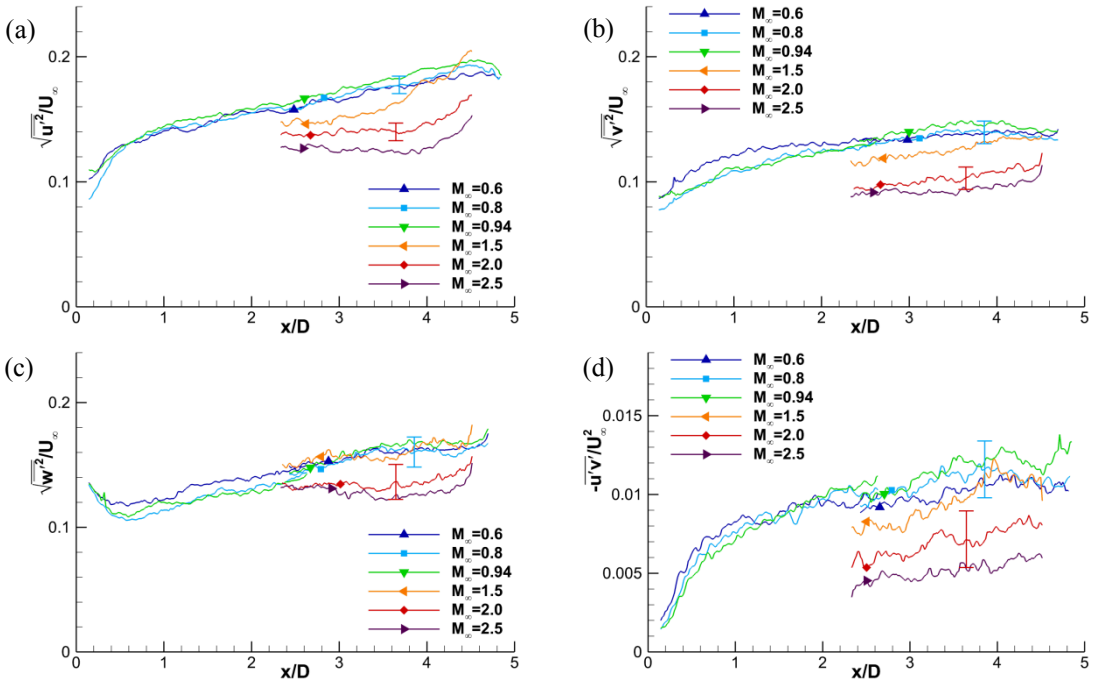

Fig. 3: As Fig. 2, but for the 5 × 3 cavity.

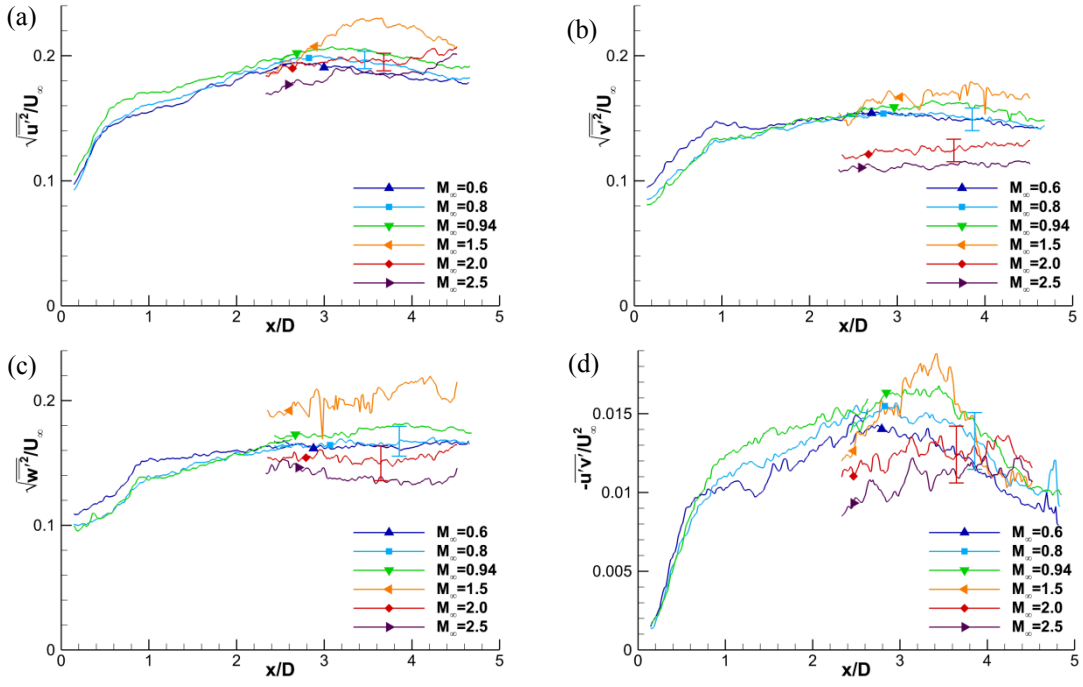

Fig. 4: As Fig. 2, but for the 5 × 1 cavity.

small. Compressibility effects in the 5 × 3 cavity are stronger than in the 5 × 1 cavity.

It therefore is clear that the influence of compressibility is a function of the cavity width. This may be a manifestation of spanwise waveforms dependent on cavity width and known to influence the flow behavior [30-34,39]. In fact, even free shear layers are known to be subject to a spanwise forcing when side walls are introduced [41,42] and that the resulting amplification rate is a function of Mach number [40,49]. This would be consistent with the presently observed behavior for a shear layer subject to the confines of a cavity and it indicates the presence of an additional instability whose susceptibility to compressibility effects may differ

from the usual shear layer instabilities. Moreover, the strength of this instability appears to be dependent upon its wavelength corresponding to the cavity width [34,50] or that different oscillatory modes emerge based on the width [51,52]. Either of these views would offer a mechanism wherein compressibility becomes a function of cavity width. Though the present measurements do not provide direct evidence of this spanwise instability, the effects on the mean flowfield structure have been observed previously [43,44] and a width dependence for the turbulence amplification is consistent. It is not clear how the presence of spillage vortices may interact with spanwise instabilities.

The only experiment known to study variation in the turbulence field of a cavity flow as a function of Mach number is Murray et al [10]. However, they study Mach numbers reaching only 0.73 and they find that v' and $u'v'$ both rise somewhat as the Mach number increases. This trend is in contrast not only with the present measurements but also with a wealth of knowledge from free shear layer experiments [12]. Furthermore, the free shear layer studies suggest that no noticeable compressibility effect should be observed until the convective Mach number reaches 0.6, which would not have been the case for Murray et al's experiment. The trends in Murray et al [10] may actually be with rising Reynolds number rather than rising Mach number, as their experiment did not decouple these parameters.

Lacking sufficient data from cavity flows, comparison with free shear layers may prove informative. Firstly, no compressibility effects are found in the turbulence quantities for the three transonic conditions. Free shear layer studies have suggested that the influence of compressibility should not occur until a convective Mach number M_c of 0.6 has been reached [16,18,19]. In the present case, M_c=0.6 is achieved between Mach 0.94 and Mach 1.5 (see the analysis in the following section) and therefore it should be expected that compressibility effects will not be observed until supersonic conditions are tested.

The prevailing view from free shear layer studies is that v' and $u'v'$ are considerably diminished as the Mach number increases but u' falls only slightly or not at all [20,22-24]. The spanwise component w' appears to remain constant [21]. The present measurements in a cavity shear layer show limited consistency with the free shear layer observations. In the 5 × 5 cavity, where the weakest compressibility influence is found, v' is the only component to show an effect. This would seem to be consistent with free shear layer data that show this component to be the most strongly affected by compressibility even if the magnitude of the effect is considerably different. The $u'v'$ values do not show a reduction with Mach number as would be suggested by comparison to free shear layers. In contrast, the 5 × 3 cavity shows a much stronger compressibility effect but a similar degree of impact is found on all three components of turbulent intensity rather than a concentration in v'. The behavior of the 5 × 1 cavity is more akin to the 5 × 3 than the 5 × 5 cavity. Overall, the trends in the cavity shear layer are not well predicted by those in a free shear layer.

The poor comparison of the turbulent stresses in a cavity shear layer to those in a free shear layer may be because different physical phenomena are at play. The canonical free shear layer is a self-similar flow. The cavity shear layer is not due to the spatially-varying lower boundary condition imposed by the recirculation region. Furthermore, free shear layers are subject to boundary conditions that are invariant in the spanwise direction whereas the present cavity flow not only has sidewall effects but also the structure and strength of the recirculation region is a function of the cavity width [43,44]. Therefore similarity should not be expected even between the different cavity geometries. Indeed, Figs. 2-4 demonstrate that the reduction in turbulence magnitudes with rising Mach number is very different for the three cavity widths that have been tested. As already noted, the interplay between the wavelength of spanwise instabilities and the cavity width is known to affect spanwise flow structure and the amplification of resonances; perhaps its influence may be found in turbulent stresses as well.

Shear Layer Growth Rates

Studies of free shear layers have shown that compressibility leads to a thinning of its vertical extent and a reduction of its growth rate (see the discussion in the Introduction). Much of the seminal research has determined the thickness of a free shear layer using a threshold rule, in which the thickness of the shear layer is determined between fixed percentage levels of each of the two freestream values. In the case of a cavity shear layer, an ambiguity arises from the presence of the recirculation region on the lower side rather than the uniform stream of a free shear layer. This presents a complication in the selection of an appropriate boundary value, which furthermore will vary along the streamwise axis.

A better approach in cavity flows is the vorticity thickness [27], $\delta_\omega = (U_1 - U_2) / (\mathrm{d}U/\mathrm{d}y)_{max}$. The use of the velocity gradient presents an unambiguous measure of the thickness without need to consider a boundary

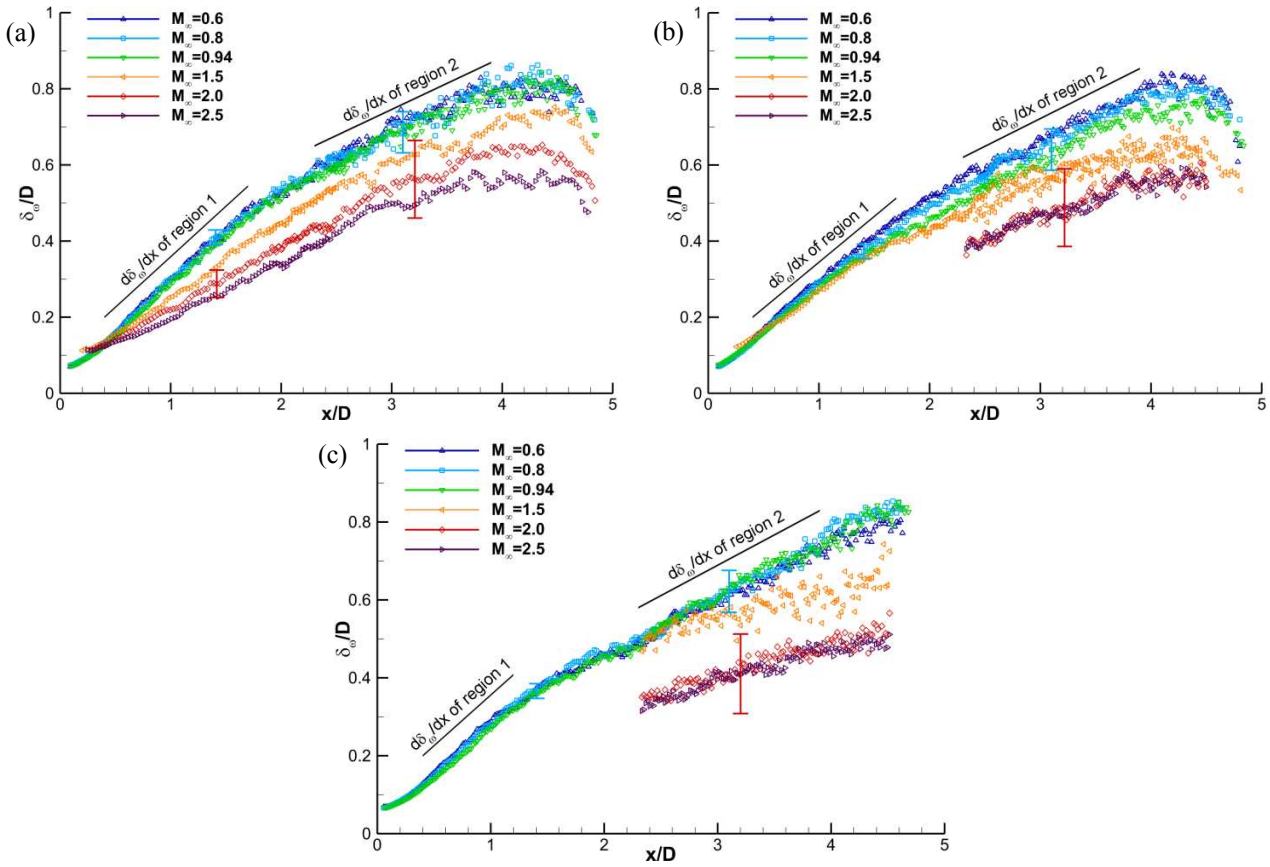

Fig. 5: Vorticity thickness of the cavity shear layer. Black lines indicate slopes of the region 1 and region 2 growth rates. (a) 5 × 5 cavity; (b) 5 × 3 cavity; (c) 5 × 1 cavity.

threshold. However, a value must be assumed for the lower stream, conventionally achieved simply by setting $U_2 = 0$ [10,53-56]. Of course, $U_1 = U_\infty$. The vorticity thickness has the additional advantage for the present experiment that it does not require measurement of the velocity field all the way to the floor of the cavity. The maximum velocity gradient can be expected near the center of the shear layer and no further penetration into the cavity is necessary. This means that the two-component measurements from the supersonic experiments and the stereoscopic measurements for the 5 × 1 cavity are all sufficient to provide an objective measure of the shear layer thickness.

Figure 5a shows the vorticity thicknesses for the 5 × 5 cavity at all six Mach numbers as a function of streamwise position in the cavity. Data are available at every x location even for the supersonic cases because the two-component measurements cover the full length of the cavity at this width. Figure 5b provides the equivalent data for the 5 × 3 cavity but here two-component data exist only for Mach 1.5 amongst the supersonic cases. Therefore, only a limited portion of the cavity has been measured using the stereoscopic data for Mach 2 and 2.5. Finally, Fig. 5c shows the vorticity thicknesses for the 5 × 1 cavity, which has no two-component measurements extending the field of view for the supersonic cases.

The vorticity thickness profiles for the 5 × 5 cavity of Fig. 5a show several features consistent with previous cavity studies. The shear layer properties may be broken into three regions based on vorticity thickness behavior [57], though some earlier studies have regarded these as only two regions by excluding the rapid decay in thickness near the aft wall [33,55,58]. The first region is characterized by fast growth of the shear layer, then the growth slows significantly to mark the onset of the second region, which extends until the aft wall influence is felt. The rapid initial growth of the shear layer is fed by the cavity's acoustic resonances exciting the Kelvin-Helmholtz instability [26,27]. At some point, this instability saturates and the growth of the shear layer tapers off to a lower but approximately constant value, accounting for region 2 [58]. An

outlying simulation finds a higher growth rate for the second stage [33]. Some incompressible or weakly compressible cavity flows have measured only a single region of growth, but these appear to occur predominately when conditions create self-sustained oscillations but do not induce resonance [53,54,56,59].

Figure 5a reveals clear differences in the growth of the 5 × 5 cavity shear layer as a function of Mach number. The three transonic cases all are essentially identical, but compressibility effects become evident for the supersonic cases. In region 1, increasing supersonic Mach number leads to a reduction of the shear layer growth rate. Conversely, region 2 appears to display less dependence on Mach number, but the overall thickness of the shear layer remains reduced at higher Mach numbers due to the continuing impact of region 1. The behavior in region 1 is precisely that which has been well established from numerous compressible free shear layer experiments. No effect comparable to region 2 is found from free shear layer studies since the latter do not exhibit saturation of the shear layer instability as may occur in cavity flows.

Data for the 5 × 3 cavity are supplied in Fig. 5b and they exhibit some differences in comparison to the 5 × 5 cavity. Region 1 measurements are not available for the two higher Mach numbers, but the transonic data alone suggest a different trend. Whereas the 5 × 5 cavity did not show any change in the region 1 growth rate for the three transonic cases, the 5 × 3 cavity suggests a diminishing growth rate as the transonic Mach number is increased. The single available supersonic case continues this trend. In region 2, growth rates are all approximately equal, as was also the case for the 5 × 5 cavity. The lower overall vorticity thicknesses for Mach 2 and Mach 2.5 in region 2, despite common slopes, suggests that the growth rate in region 1 must have been lower still for these cases.

The behavior of the 5 × 1 cavity is again different. Here, the region 1 growth rates are identical for the three transonic cases, but the region 2 growth rates appear to show lower values for the supersonic cases as compared to transonic. Moreover, region 1 terminates earlier than for the 5 × 5 and 5 × 3 cavities, suggesting that the instability saturates more rapidly. The 5 × 1 data do not extend quite as far downstream as for the two wider cavities because the limited depth interferes with evaluation of the vorticity thickness near the aft wall.

The growth rates may be found by determining the slopes of the vorticity thickness plots in each of the first two regions. The region 1 growth rates should be most comparable to the growth rates of free shear layers, as this is the portion of the flow prior to saturation of the instability, which does not occur in free shear layers. Region 1 is defined as $0.4 < x/D < 1.7$ for the 5 × 5 and 5 × 3 cavities but shortened to $0.4 < x/D < 1.2$ for the 5 × 1 cavity, based on linearity of the plots in Fig. 5. A simple least-squares fit was used to calculate the shear layer growth rate $d\delta_\omega/dx$.

Also needed for comparison to free shear layers is to cast the data in terms of the convective Mach number, M_c, rather than the freestream Mach number. Studies of free shear layers have well established that use of the convective Mach number of the flow better establishes similarity [11-13]. The convective Mach number is more difficult to determine in the present case because the slow side of the shear layer is bounded by the recirculation region in the cavity as opposed to a uniform freestream, but the assumption of $U_2 = 0$ that was used to calculate the vorticity thickness may be redeployed here. A similar difficulty is encountered in the shear layer over a base flow and the convective Mach number still can be reasonably estimated to find similarity in the data [12].

To properly assess the effect of compressibility on the shear layer growth rate, it must be normalized to its incompressible value. This poses something of a challenge in the present case given that the experiments were conducted exclusively in the compressible regime and no other known incompressible cavity experiments exactly replicate the current finite-width geometries. This is an important consideration, as the current data have shown that the changes to the cavity width affect the shear layer properties. Moreover, as Murray et al [10] point out, incompressible cavities of the current dimensional range often do not resonate, and this appears to alter the shear layer growth rate.

The growth rates found in Figs. 2 and 4 for transonic cases suggest that a reasonable choice of the incompressible cavity growth rate in region 1 can be chosen as 0.26 because compressibility effects have not yet established an influence on the shear layer. An extrapolation of the transonic influence on growth rates in Fig. 3 is consistent. This value is used to normalize the measured compressible shear layer growth rates. The normalized growth rate $\Phi = (d\delta_\omega/dx) / (d\delta_\omega/dx)_{incompressible}$ and is plotted as a function of M_c.

Figure 6 reproduces the compilation of Smits and Dussauge [13], which is probably the most complete survey of the available data. Growth rates may differ somewhat from the values reported by the original authors as Smits and Dussauge incorporate subsequent reassessments of the data. The trend of decreasing

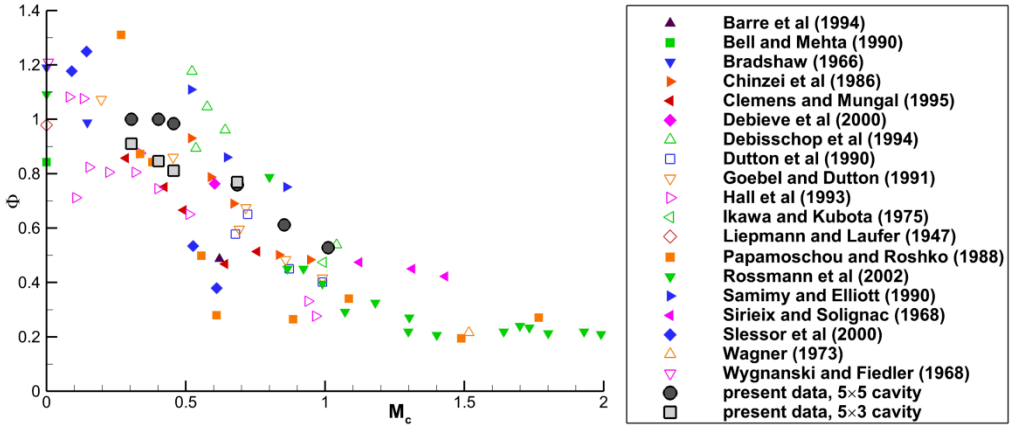

Fig. 6: Normalized growth rates of region 1 of the cavity shear layer as a function of convective Mach number, superposed on values from free shear layers. After Smits and Dussauge [13].

normalized growth rate with convective Mach number is strongly evident, even within the substantial scatter of the data. Some of this scatter is attributable to the disparate experimental means of measuring the shear layer thickness [13,60].

The present cavity data are superposed on the free shear layer data in Fig. 6. Region 1 growth rates are comparable to those from free shear layers because the physical processes are expected to be similar before the instability saturates in region 2, which is not known to occur in free shear layers. The most complete data are those for the 5 × 5 cavity and these are observed to faithfully follow the free shear layer trends. The three transonic cases show minimal variation in growth rate, but once supersonic conditions are reached a considerable reduction in growth rate occurs as the Mach number rises. The 5 × 3 cavity differs in that the transonic growth rates are lower than those of the 5 × 5 cavity and show a diminishing trend with increased Mach number even at these weakly compressible conditions. The single data point for a supersonic case in the 5 × 3 cavity closely matches its 5 × 5 counterpart. Despite the earlier onset of a growth rate reduction, the 5 × 3 cavity data also are well within the bounds of the free shear layer data. The 5 × 1 case is excluded because region 1 measurements are not available for Mach numbers at which compressibility effects are observed; the available transonic cases closely match the 5 × 5 data points. Smits and Dussauge [13] noted that shear layer thicknesses determined using the velocity field tend to produce values of Φ towards the higher end of the scatter, and in fact the present measurements lie somewhat greater than the general centroid of the data points. Therefore, the classic compressibility effect on free shear layer growth has been confirmed in the present cavity shear layer data as well. It is interesting to note that the cavity shear layer growth rates well match those from free shear layers despite the absence of good agreement in the turbulence quantities analyzed in Figs. 2-4.

Free shear layer studies have suggested that the compressible reduction of shear layer growth occurs predominantly above M_c=0.6, at which point the instability mechanism may shift away from the classic Kelvin-Helmholtz instability [16,18,19]. This appears to be the case for the present cavity data as well, but only for the 5 × 5 cavity. The 5 × 3 cavity is not consistent with this trend and displays a falling growth rate across all measured Mach numbers, which may suggest a different instability is operative for this cavity width. The inference of a stronger spanwise instability in the 5 × 3 cavity would be supported by the earlier observations regarding turbulent stresses in Figs. 2-4.

Conclusions

The present paper gathers data from two previous experiments studying compressible flow over a rectangular cavity using two-component and stereoscopic particle image velocimetry. A range of freestream Mach numbers from 0.6 to 2.5 has been studied, which corresponds to an estimated convective Mach number of the cavity shear layer reaching 1.01. These data offer an opportunity to explore the influence of compressibility on the turbulence properties of the cavity shear layer and compare the results to those known for free shear layers.

Mean velocity fields reveal that the structure of the recirculation region is essentially invariant with Mach number but differs for the three cavity widths. Measurements of the turbulent stresses also show different behavior based on cavity width. The widest cavity exhibits a significant compressibility effect only in the vertical component of the turbulence intensity, in which values of this term diminish modestly as Mach number rises. The two narrower cavities show a more substantial drop in all three components of the turbulence intensity as well as the turbulent shear stress. These observations stand in contrast to velocimetry measurements made in canonical free shear layers, which show that the vertical component and the turbulent shear stress are reduced as the Mach number increases but the streamwise and spanwise components are minimally affected [20-24]. The relative importance of a spanwise instability may explain the dependence of compressibility effects upon the cavity width. One similarity between free shear layers and cavity shear layers is that these compressibility effects on turbulence quantities are initiated only once the convective Mach number exceeds approximately 0.6.

The growth of the cavity shear layer was determined using mean streamwise velocity fields. The vorticity thickness grows rapidly as the shear layer initially develops, then transitions to a slower growth rate once its instability saturates; finally, it falls quickly when the aft wall is neared. Growth rates are approximately constant with streamwise distance in each region and were calculated from the slope of the vorticity thickness. The initial growth rate in the widest cavity falls sharply as a function of Mach number once a convective Mach number of 0.6 is surpassed, but an onset of the growth rate reduction below this Mach number is possible for a narrower cavity. Post-saturation growth rates are approximately constant with Mach number for all three cavity widths. The growth rates prior to saturation were normalized by their estimated incompressible values and plotted against convective Mach number. Showing excellent agreement with the comparable free shear layer data compiled by Smits and Dussauge [13], the cavity shear layer displays the classic compressibility effect of suppression of its growth rate as the convective Mach number rises. The specific trend of the reduction in growth rate due to compressibility is modified by the cavity width.

References

[1] TRACY, M. B., and PLENTOVICH, E. B. 1997 Cavity unsteady-pressure measurements at subsonic and transonic speeds. NASA Technical Paper 3669.

[2] STALLINGS, R. L., and WILCOX, F. J. 1987 Experimental cavity pressure distributions at supersonic speeds. NASA Technical Paper 2683.

[3] ROSSITER, J. E. 1964 Wind-tunnel experiments on the flow over rectangular cavities at subsonic and transonic speeds. Aeronautical Research Council Report 3438.

[4] HELLER, H. H., and BLISS, D. B. 1975 The physical mechanism for flow-induced pressure fluctuations in cavities and concepts for their suppression. *AIAA Paper* 75-491.

[5] CLARK, R. L., KAUFMAN, L. G. II, and MACIULAITUS, A. (1980) Aeroacoustic measurements for Mach .6 to 3.0 flows past rectangular cavities. *AIAA Paper* 80-0036.

[6] MALONE, J., DEBIASI, M., LITTLE, J., and SAMIMY, M. 2009 Analysis of the spectral relationships of cavity tones in subsonic resonant cavity flows. *Physics of Fluids* **21**(5), 055103.

[7] ZHANG, X., and EDWARDS, J. A. 1990 An investigation of supersonic oscillatory cavity flows driven by thick shear layers. Aeronautical *Journal* **94**(940) 355-364.

[8] MURRAY, R. C., and ELLIOTT, G. S. 2001 Characteristics of the compressible shear layer over a cavity. *AIAA Journal* **39**(5) 846-856.

[9] UNALMIS, O. H., CLEMENS, N. T., and DOLLING, D. S. 2004 Cavity oscillation mechanisms in high-speed flows. *AIAA* Journal **42**(10), 2035-41.

[10] Murray, N., SALLSTROM, E., and UKEILEY, L. 2009 Properties of subsonic open cavity flow fields. *Physics of Fluids* **21**(9), 095103.

[11] LELE, S. K. 1994 Compressibility Effects in Turbulence. *Annual Review of Fluid Mechanics* **26**, 211-254.

[12] DUTTON, J. C. 1997 Compressible Turbulent Free Shear Layers. AGARD Report 819: *Turbulence in Compressible* Flows, 2-1 to 2-42.

[13] SMITS, A. J., and DUSSAUGE, J.-P. 2006 *Turbulent Shear Layers in Supersonic Flow*, 2nd ed., Springer, NY, 139-178.

[14] PAPAMOSCHOU, D., and ROSHKO, A. 1988 The compressible turbulent shear layer: an experimental study. *Journal of Fluid Mechanics* **197**, 453-477.

[15] HALL, J. L., DIMOTAKIS, P. E., and ROSEMANN, H. 1993 Experiments in nonreacting compressible shear layers. *AIAA Journal* **31**(12), 2247-2254.

[16] CLEMENS, N. T., and MUNGAL, M. G. 1995 Large-scale structure and entrainment in the supersonic mixing layer. *Journal of Fluid Mechanics* **284**, 171-216.

[17] ROSSMANN, T., MUNGAL, M. G., and HANSON, R. K. 2002 Evolution and growth of large-scale structures in high compressibility mixing layers. *Journal of Turbulence* **3**(1), 9.
[18] ELLIOTT, G. S., SAMIMY, M., and ARNETTE, S. A. 1995 The characteristics and evolution of large-scale structures in compressible mixing layers. *Physics of Fluids* **7**(4), 864-876.
[19] SANDHAM, N. D., and REYNOLDS, W. C. 1991 Three-dimensional simulations of large eddies in the compressible mixing layer. *Journal of Fluid Mechanics* **224**, 133-158.
[20] GOEBEL, S. G., and DUTTON, J. C. 1991 Experimental study of compressible turbulent mixing layers. *AIAA Journal* **29**(4), 538-546.
[21] GRUBER, M. R., MESSERSMITH, N. L., and DUTTON, J. C. 1993 Three-dimensional velocity field in a compressible mixing layer. *AIAA Journal* **31**(11), 2061-2067.
[22] ELLIOTT, G. S., and SAMIMY, M. 1990 Compressibility effects in free shear layers. *Physics of Fluids A* **2**(7), 1231-1240.
[23] FREUND, J. B., LELE, S. K., and MOIN, P. 2000 Compressibility effects in a turbulent annular mixing layer. Part 1. Turbulence and growth rate. *Journal of Fluid Mechanics* **421**, 229-267.
[24] URBAN, W. D., and MUNGAL, M. G. 2001 Planar velocity measurements in compressible mixing layers. *Journal of Fluid* Mechanics **431**, 189-222.
[25] OLSEN, M. G., and DUTTON, J. C. 2003 Planar velocity measurements in a weakly compressible mixing layer. *Journal of Fluid* Mechanics **486**, 51-77.
[26] GHARIB, M., and ROSHKO, A. 1987 The effect of flow oscillations on cavity drag. *Journal of Fluid Mechanics* **177**, 501-530.
[27] ROWLEY, C. W., COLONIUS, T., and BASU, A. J. 2002 On self-sustained oscillations in two-dimensional compressible flow over rectangular cavities. *Journal of Fluid Mechanics* **455**, 315-346.
[28] ROCKWELL, D., and KNISELY, C. 1979 The organized nature of flow impingement upon a corner. *Journal of Fluid Mechanics* **93**(3) 413-432.
[29] LIU, X., and KATZ, J. 2013 Vortex-corner interactions in a cavity shear layer elucidated by time-resolved measurements of the pressure field. *Journal of Fluid Mechanics* **728**, 417-457.
[30] MAULL, D. J., and EAST, L. F. 1963 Three-dimensional flow in cavities. *Journal of Fluid Mechanics* **16**, 620-632.
[31] ROCKWELL, D., and KNISELY, C. 1980 Observations of the three-dimensional nature of unstable flow past a cavity. *Physics of* Fluids **23**(3), 425-431.
[32] LARCHEVÊQUE, L., SAGAUT, P., and LABBÉ, O. 2007 Large-eddy simulation of a subsonic cavity flow including asymmetric three-dimensional effects. *Journal of Fluid Mechanics* **577**, 105-126.
[33] BRÈS, G. A., and COLONIUS, T. 2008 Three-dimensional instabilities in compressible flow over open cavities *Journal of Fluid* Mechanics **599**, 309-339.
[34] FAURE, T. M., Pastur, L., LUSSEYRAN, F., FRAIGNEAU, Y., and BISCH, D. 2009 Three-dimensional centrifugal instabilities development inside a parallelepipedic open cavity of various shape. *Experiments in Fluids*, **47**(3) 395-410.
[35] BASLEY, J., PASTUR, L. R., DELPRAT, N., and LUSSEYRAN, F. 2013 Space-time aspects of a three-dimensional multi-modulated open cavity flow. *Physics of Fluids* **25**(6), 064105.
[36] AHUJA, K. K., and MENDOZA, J. 1995 Effects of cavity dimensions, boundary layer, and temperature on cavity noise with emphasis on benchmark data to validate computational aeroacoustic codes. NASA Contractor Report 4653.
[37] DISIMILE, P. J., TOY, N., and SAVORY, E. 2000 Effect of planform aspect ratio on flow oscillations in rectangular cavities. *Transactions of the ASME* **122**(1), 32-38.
[38] CHUNG, K.-M. 2001 Three-dimensional effect on transonic rectangular cavity flows. *Experiments in Fluids* **30**(5), 531-536.
[39] ZHANG, K., and NAGUIB, A. M. 2011 Effect of finite cavity width on flow oscillation in a low-mach-number cavity flow. Experiments *in Fluids* **51**(5), 1209-1229.
[40] ZHUANG, M., DIMOTAKIS, P. E., and KUBOTA, T. 1990 The effect of walls on a spatially growing supersonic shear layer. Physics *of Fluids A* **2**(4), 599-604.
[41] MORRIS, P. J., and GIRIDHARAN, M. G. 1991 The effect of walls on instability waves in supersonic shear layers. *Physics of Fluids A* **3**(2), 356-358.
[42] CLEMENS, N. T., and MUNGAL, M. G. 1992 Effects of sidewall disturbances on the supersonic mixing layer. *AIAA Journal* **8**(1), 249-251.
[43] BERESH, S. J., WAGNER, J. L., PRUETT, B. O. M., HENFLING, J. F., and SPILLERS, R. W. 2015 Supersonic flow over a finite-width rectangular cavity. *AIAA Journal* **53**(2), 296-310.
[44] BERESH, S. J., WAGNER, J. L., PRUETT, B. O. M., HENFLING, J. F., and SPILLERS, R. W. 2015 Width effects in transonic flow over a rectangular cavity. *AIAA Journal* **53**(12), 3831-3834.
[45] WAGNER, J. L., CASPER, K. M., BERESH, S. J., HENFLING, J. F., SPILLERS, R. W., and PRUETT, B. O. M. 2015 Mitigation of wind tunnel wall interactions in subsonic cavity flows. *Experiments in Fluids* **56**(3), 59.
[46] ZHUANG, N., ALVI, F. S., ALKISLAR, M. B., and SHIH, C. 2003 Aeroacoustics properties of supersonic cavity flows and their control. AIAA Paper 2003-3101.
[47] GAI, S. L., KLEINE, H., and NEELY, A. J. 2015 Supersonic flow over a shallow open rectangular cavity. *Journal of Aircraft*, **52**(2), 609-616.
[48] WAGNER, J. L., CASPER, K. M., BERESH, S. J., HUNTER, P. S., HENFLING, J. F., SPILLERS, R. W., and PRUETT, B. O. M. 2015 Fluid-structure interactions in compressible cavity flows. *Physics of Fluids* **27**(6), 066102.
[49] ROBINET, J.-C., DUSSAUGE, J.-P., and CASALIS, G. 2001 Wall effect on the convective-absolute boundary for the compressible shear layer. *Theoretical and Computational Fluid Dynamics* **15**(3), 143-163.

[50] BASLEY, J., PASTUR, L. R., LUSSEYRAN, F., SORIA, J., and DELPRAT, N. 2014 On the modulating effect of three-dimensional instabilities in open cavity flows. *Journal of Fluid Mechanics* **759**, 546-578.
[51] DE VICENTE, J., BASLEY, J., MESEGUER-GARRIDO, F., SORIA, J., and THEOFILIS, V. 2014 Three-dimensional instabilities over a rectangular open cavity: from linear stability analysis to experimentation. *Journal of Fluid Mechanics* **748**, 189-220.
[52] DOUAY, C. L., PASTUR, L. R., and LUSSEYRAN, F. 2016 Centrifugal instabilities in an experimental open cavity flow. *Journal* of *Fluid Mechanics* **788**, 670-694.
[53] HAIGERMOSER, C., VESELY, L., NOVARA, M., and ONORATO, M. 2008 A time-resolved particle image velocimetry investigation of a cavity flow with a thick incoming turbulent boundary layer. *Physics of Fluids* **20**(10), 105101.
[54] KANG, W., LEE. S. B., and SUNG, H. J. 2008 Self-sustained oscillations of turbulent flows over an open cavity. Experiments *in Fluids* **45**(4), 693-702.
[55] BIAN, S., DRISCOLL, J. F., ELBING, B. R., and CECCIO, S. L. 2011 Time resolved flow-field measurements of a turbulent mixing layer over a rectangular cavity. *Experiments in Fluids* **51**(1), 51-63.
[56] CROOK, S. D., LAU, T. C. W., and KELSO, R. M. 2013 Three-dimensional flow within shallow, narrow cavities. *Journal of Fluid Mechanics* **735**, 587-612.
[57] FORESTIER, N., JACQUIN, L., and GEFFROY, P. 2003 The mixing layer over a deep cavity at high-subsonic speed. *Journal of Fluid Mechanics* **465**, 101-145.
[58] LARCHEVÊQUE, L., SAGAUT, P., THIEN-HIEP, L., and COMTE, P. 2004 Large-eddy simulation of a compressible flow in a three-dimensional open cavity at high Reynolds number. *Journal of Fluid Mechanics* **516**, 265-301.
[59] Ashcroft, G., and ZHANG, X. 2005 Vortical structures over rectangular cavities at low speed. *Physics of Fluids* **17**(1), 015104.
[60] BARONE, M. F., OBERKAMPF, W. L., and BLOTTNER, F. G. 2006 Validation case study: prediction of compressible turbulent mixing layer growth rate. *AIAA Journal* **44**(7), 1488-1497.